JACC: CASE REPORTS VOL. 2, NO. 10, 2020

MINI-FOCUS ISSUE: IMAGING

INTERMEDIATE

CASE REPORT: CLINICAL CASE

Roadmap to the Mechanisms of Aortic Regurgitation on Echocardiography

Karima Addetia, MD, Roberto M. Lang, MD

ABSTRACT

The purpose of this series was to improve assessment of the aortic valve by echocardiography and to encourage echocardiographers to assess the cause of aortic regurgitation. The study illustrates the use of the Carpentier classification system for classifying the causes of regurgitation with a case series. (**Level of Difficulty: Intermediate.**) (J Am Coll Cardiol Case Rep 2020;2:1589–94) © 2020 The Authors. Published by Elsevier on behalf of the American College of Cardiology Foundation. This is an open access article under the CC BY-NC-ND license (http://creativecommons.org/licenses/by-nc-nd/4.0/).

Similar to the efforts being made to describe the mechanisms of mitral regurgitation (MR), efforts are also being applied toward clarifying the cause of aortic regurgitation (AR), which could improve our understanding of aortic valve (AV) pathology. The Carpentier classification, for instance, has been applied in the planning of AV repair, directing surgeons toward more tailored approaches, resulting in improved repair durability (1). Cardiac imagers, however, have not universally adopted this schema, despite the fact that recent guidelines (2) do recommend the use of this system to classify the causes of AR. Accordingly, the purpose of this series was to encourage imagers to assess the cause of AR as they do MR by using the Carpentier classification system (**Table 1**).

LEARNING OBJECTIVES

- To recognize the importance of measuring the ventriculoaortic junction, sinus of Valsalva, and sinotubular junction in every patient with significant AR.
- To be able to use the Carpentier classification system to stipulate the cause of AR.
- To appreciate the value of 3D echocardiography in the assessment of the cause of AR.

PRESENTATION

CASE 1. A 38-year-old man with a history of poorly controlled hypertension, end-stage renal disease on dialysis, and pulmonary embolism taking warfarin therapy was admitted with congestive heart failure. Transthoracic echocardiography (TTE) performed on hospitalization day 3 showed moderate concentric left ventricular (LV) hypertrophy with an LV ejection fraction (LVEF) of 35%. There was moderate to severe AR with normal leaflet morphology (**Figure 1**, far left). Both the sinus of Valsalva (SoV) and the

From the Section of Cardiology, Department of Medicine, University of Chicago, Chicago, Illinois. Dr. Lang serves on the Speakers Bureau and advisory bureau, and has received research grants from Philips Medical Imaging. All other authors have reported that they have no relationships relevant to the contents of this paper to disclose.

The authors attest they are in compliance with human studies committees and animal welfare regulations of the authors' institutions and Food and Drug Administration guidelines, including patient consent where appropriate. For more information, visit the *JACC: Case Reports* author instructions page.

Manuscript received June 5, 2020; revised manuscript received July 8, 2020, accepted July 13, 2020.

ISSN 2666-0849 https://doi.org/10.1016/j.jaccas.2020.07.012

ABBREVIATIONS AND ACRONYMS

AAo = ascending aorta

AR = aortic regurgitation

LV = left ventricular

LVEF = left ventricular ejection fraction

MR = mitral regurgitaton

SJ = sinotubular junction

SoV = sinus of Valsalva

TEE = transesophageal echocardiogram

TTE = transthoracic echocardiogram

VAJ = ventriculoaortic junction

ventriculoaortic junction (VAJ) were normal in size (**Figures 1A and 1B**, Video 1). The sinotubular junction (SJ) was enlarged and effaced with dilation of the ascending aorta (AAo) (**Figures 1A and 1B**) and central AR (**Figures 1C and 1D**). Given the normal aortic cusp motion and the presence of SJ and AAo dilation, this patient's AR was classified as Type Ia.

CASE 2. A 70-year-old man with a history of renal cell carcinoma status post-nephrectomy, hypertension, cerebrovascular accident, and remote myocardial infarction was referred to the cardiology clinic for aortic root dilation and AR. His only symptom was fatigue. A TTE followed by transesophageal echocardiography (TEE) revealed Type Ib AR (**Figure 2**, far left panel) with normal AV leaflets and dilation of the SoV and SJ (**Figure 2A**, Video 2). There was moderate AR by vena contracta (58 mm) (**Figure 2B**). The VAJ was within normal limits (**Figure 2C**), whereas the AAo measured 45 mm, 65 mm from the VAJ. His LVEF was 55% to 60%.

CASE 3. A 67-year-old man with a history of hypertension was being evaluated in the electrophysiology clinic for recent onset palpitations. A TTE showed Type Ic AR (**Figure 3**, far left panel) with normal AV leaflets and dilation of the VAJ (**Figure 3A**). The SoV size was borderline normal, and the SJ and AAo sizes were also normal (**Figure 3B**). There was severe AR (**Figure 3C**)

CASE 4. A 31-year-old male construction worker with a history of chronic severe AR was seen in the cardiology clinic for worsening shortness of breath. A TEE was performed as part of his work-up for possible AV repair. This patient's condition was an example of Type Id AR (**Figure 4**, far left panel). The SoV, SJ, and VAJ were within normal limits (**Figures 4A and 4B**), but there was clear perforation of the noncoronary cusp (**Figures 4C and 4D**, blue arrows, Video 3). This was seen on the 2-dimensional (2D) mid-esophageal short-axis view of the AV (**Figures 4E and 4F**, blue arrow), on the 3D narrow-angle imaging captured in end-systole (**Figure 4G**, blue arrow), and on 3D color Doppler imaging, also captured in end-systole (**Figure 4H**, blue arrow).

CASE 5. A 49-year-old man with a history of hypertension, diabetes, and hyperlipidemia with asymptomatic chronic AR (until the current admission when he presented with congestive heart failure). The patient's TEE was obtained to determine the mechanism of AR. This patient's condition is an example of Type II AR (**Figure 5**, far left panel), associated with excess leaflet motion. The SoV, SJ, and VAJ were dilated (**Figure 5A**). There was prolapse of the right coronary cusp (**Figures 5B and 5C**, yellow R, Video 4). The resultant AR was eccentric and directed toward the anterior mitral valve leaflet (**Figure 5D**). The predominant cause of AR was right coronary cusp prolapse (Type II) with associated Type I disease.

CASE 6. A 67-year-old healthy man with asymptomatic chronic moderate AR was being followed on a regular basis until he developed a drop in LVEF on TTE. A TEE was ordered to better assess AR severity. The TEE revealed Type III severe AR (**Figure 6**, far left). The SoV was mildly dilated. The SJ and VAJ were normal in size (**Figure 6A**). The AAo was 42 mm (mildly dilated). The AV leaflets were thickened and restricted on 2D imaging (**Figure 6B**), resulting in malcoaptation and AR (**Figure 6C**). The leaflet thickening and restriction was clearly observed on the 3D narrow-angle image taken in end-diastole (**Figure 6D**).

TABLE 1 Carpentier Classification of Aortic Regurgitation

AR Type	Aortic Annulus	Sinus of Valsalva	Sinotubular Junction	Ascending Aorta	Other
Normal Leaflets					
Type Ia	↔	↔	↑↑	↑↑	-
Type Ib	↔	↑↑	↑↑	↔	-
Type Ic	↑↑	↔	↔	↔	-
Type Id	↔	↔	↔	↔	Perforation
Type II	↔	↔	↔	↔	Cusp prolapse
Type III	↔	↔	↔	↔	Cusp restriction

↔ Denotes that the measurement could be increased/decreased or normal.
AR = aortic regurgitation.

FIGURE 1 **Type Ia AR Is Associated With Dilation of the AAo and SJ**

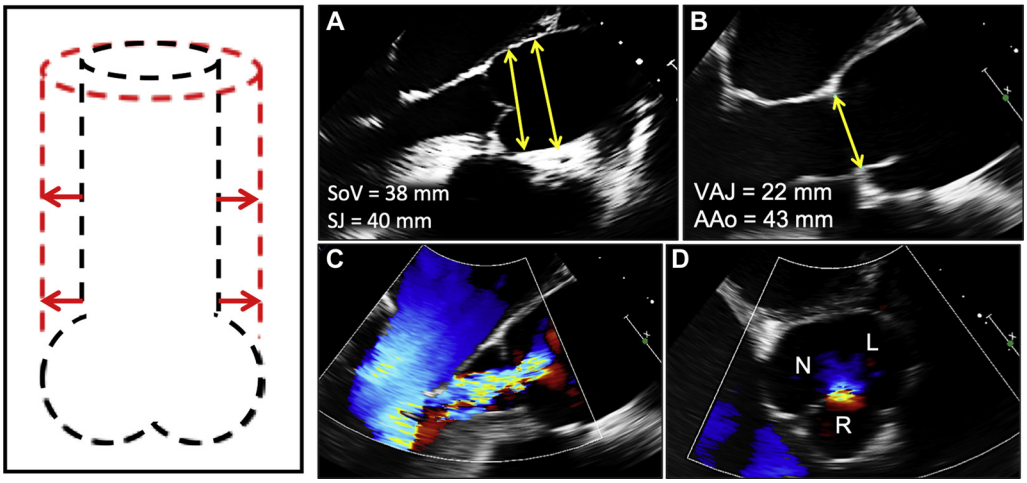

Schematic showing the outline of a normal aortic root and ascending aorta **(black)** and changes expected in Type Ia aortic regurgitation (AR) (i.e., a dilated sinotubular junction [SJ] and ascending aorta [AAo]) **(left panel)**. On the **right**, 2-dimensional and color Doppler images of the aortic root in a patient with Type 1a AR **(A to D)**. See text for details. L = left coronary cusp; N = non-coronary cusp; R = right coronary cusp; SoV = sinus of Valsalva; VAJ = ventriculoaortic junction.

Figures 6E to 6G show systolic frames of the AV from the aortic perspective (Figure 6E), the LV outflow tract perspective (Figure 6F), and with 3D color Doppler from the aortic perspective (Figure 6G). All 3D narrow-angle datasets (Figures 6D to 6F, Video 5) confirmed thickening of the free margin on the leaflets. Normally, aortic leaflets are thin and difficult to image on 3D. Here the leaflets were not

FIGURE 2 **Type Ib AR Is Associated With Dilation of the SoV and SJ**

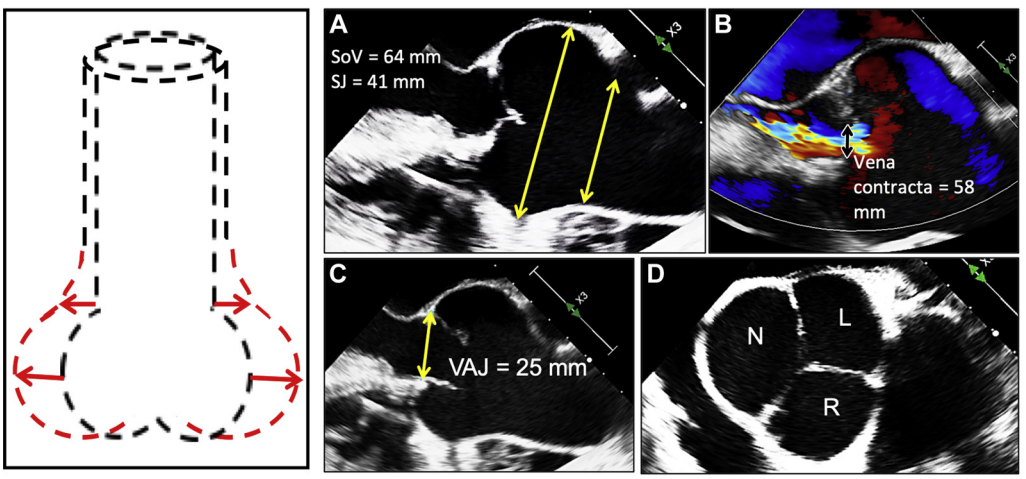

Schematic showing the outline of a normal aortic root and ascending aorta **(black)** and changes expected in Type Ib AR (i.e., a dilated SoV and SJ) **(left panel).** On the **right,** 2-dimenstsional and color Doppler images of the aortic root in a patient with Type 1b AR **(A to D)**. See text for details. Abbreviations as in Figure 1.

FIGURE 3 Type Ic AR Is Associated With Dilation of the VAJ

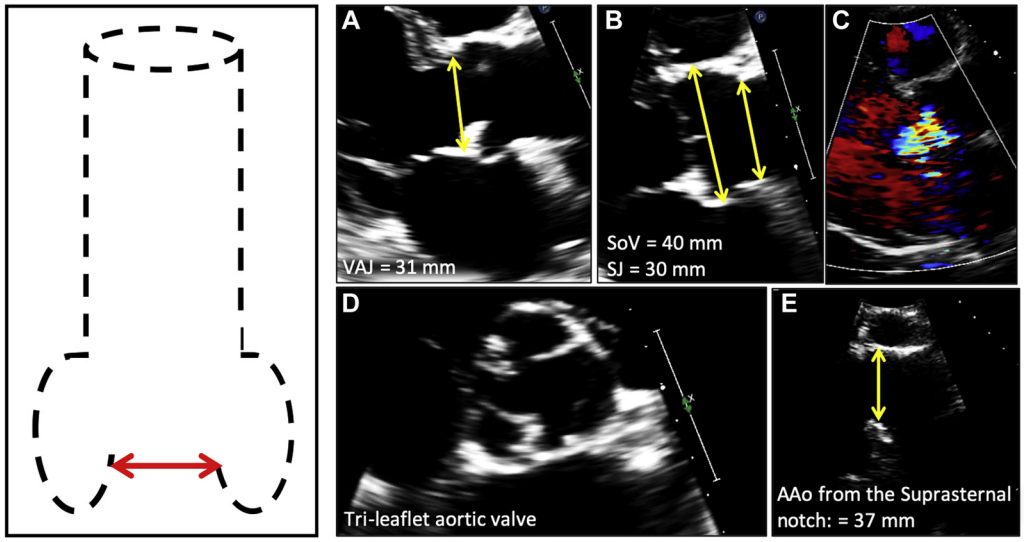

Schematic showing the outline of a normal aortic root and ascending aorta **(black)** and changes expected in Type Ic AR related to dilation of the VAJ **(left panel)**. On the **right,** 2-dimenstional and color Doppler images of the aortic root in a patient with Type 1c AR **(A to E)**. See text for details. Abbreviations as in Figure 1.

translucent and were seen in their entirety on 3D imaging due to the abnormal thickening. A 3D color Doppler confirmed the fact that the origin of the AR was the area of malcoaptation (Figure 6G), which seems to be in the middle of all 3 leaflets.

DISCUSSION

The AV is part of the aortic root (Figure 7). The VAJ forms the basal attachment of the AV cusps and denotes the aortic annulus. The SJ forms the proximal

FIGURE 4 Type Id AR Is Associated With Leaflet Perforation

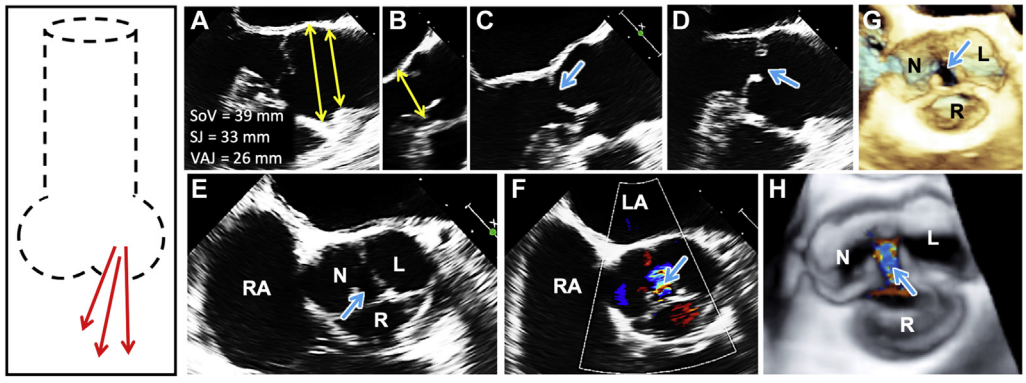

Schematic showing the outline of the aortic root and ascending aorta **(black)** and changes expected in Type Id AR (i.e., perforation of the aortic valve leaflet) **(left panel)**. On the **right,** 2-dimensional, 2-dimensional color Doppler, 3-dimensional narrow-angle, and 3-dimensional color Doppler images of the aortic root are depicted in a patient with Type 1d AR **(A to H)**. **Blue arrows** identify the area of leaflet perforation in the noncoronary cusp. See text for details. Abbreviations as in Figure 1.

FIGURE 5 Type II AR Is Associated With Excessive Leaflet Motion

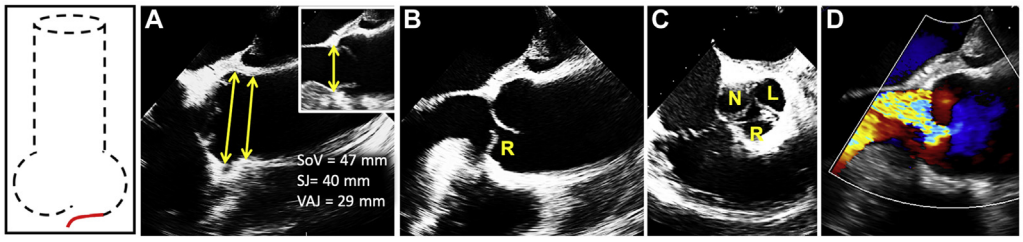

Schematic showing the outline of the aortic root and ascending aorta **(black)** and changes expected in Type II AR (i.e., leaflet prolapse) in **red (left panel)**. On the **right,** 2D and color Doppler images of the aortic root are depicted in a patient with Type II AR **(A to D).** See text for details. Abbreviations as in Figure 1.

border of the aortic root. The valve leaflets extend from the aortic annulus to the SJ within the SoV in a "crown-like" formation. Type Ia AR is characterized by dilation of the SJ, Type Ib AR by dilation of the SoV and SJ, whereas dilation of the VAJ is noted in Type Ic AR. Note that dilation of the AAo alone will not cause AR unless it is coupled with dilation of the SJ. Type Id AR is associated with leaflet perforation. Type II is due to excessive leaflet motion (e.g., prolapse) or loss of commissural integrity and type III AR to leaflet restriction and sometimes commissural fusion (e.g., bicuspid aortic valve disease, rheumatic aortic valve disease).

Application of the Carpentier classification system to the dysfunctional MV has improved interdisciplinary communication and decision making regarding options for managing MR. Recent surgical studies have supported the use of the Carpentier

FIGURE 6 Type III AR Is Associated With Leaflet Restriction

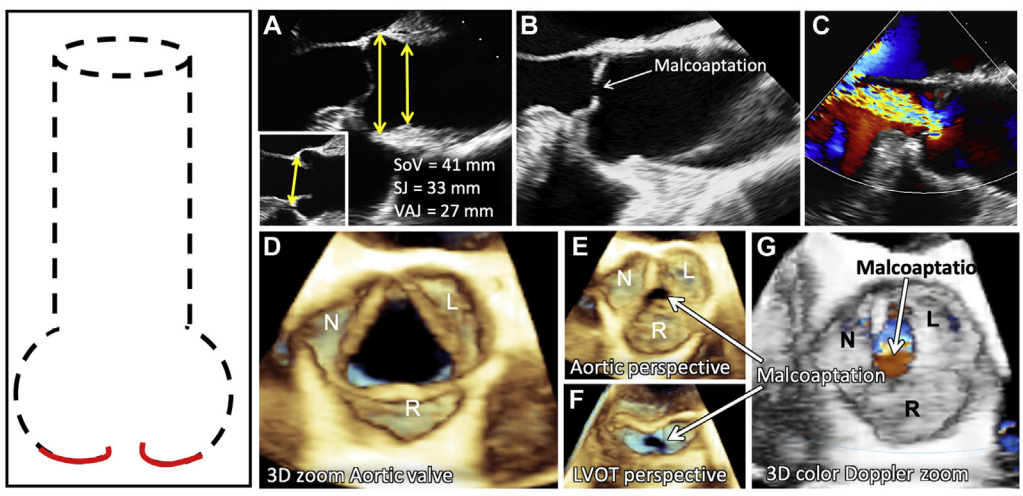

Schematic showing the outline of the aortic root and ascending aorta **(black)** and changes expected in Type III AR (i.e., restricted leaflet motion) **(left panel)**. On the **right,** 2-dimensional, 2-dimensional color Doppler, 3-dimensional narrow-angle, and 3-dimensional color Doppler images of the aortic root are depicted in a patient with Type III AR **(A to G)**. **White arrows** identify the area of leaflet malcoaptation shown in the end-systolic frame. See text for details. LVOT = left ventricular outflow tract; other abbreviations as in Figure 1.

FIGURE 7 Diagram of the Aortic Root

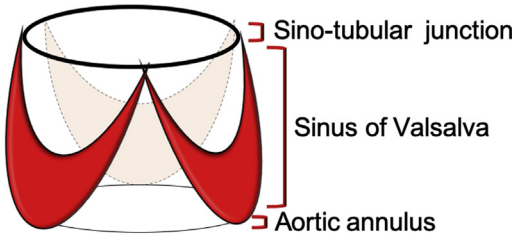

See text for details.

classification system for AR, suggesting that it could help the surgeon optimize the selection of repair techniques and predict the durability of these techniques (1,3). Both Types I and II AR have been shown to have better post-repair outcomes than Type III AR, suggesting that leaflet restriction causing AR is the most challenging type to repair.

CONCLUSIONS

As imagers, we spend less time characterizing AR lesions than we do MR lesions. The Carpentier classification illustrated with cases here was pioneered by surgeons in the operating theater to help guide AV repair. Adopting this schema in echocardiography laboratories for AR could help unify the way we report classifications of AR and advance the way we think about this lesion.

ADDRESS FOR CORRESPONDENCE: Dr. Karima Addetia, Section of Cardiology, University of Chicago Medical Center, 5842 South Maryland Avenue, MC 9067, Chicago, Illinois 60637. E-mail: kaddetia@medicine.bsd.uchicago.edu.

REFERENCES

1. Boodhwani M, de Kerchove L, Glineur D, et al. Repair-oriented classification of aortic insufficiency: impact on surgical techniques and clinical outcomes. J Thorac Cardiovasc Surg 2009;137:286–94.

2. Zoghbi WA, Adams D, Bonow RO, et al. Recommendations for noninvasive evaluation of native valvular regurgitation: a report from the American Society of Echocardiography developed in collaboration with the Society for Cardiovascular Magnetic Resonance. J Am Soc Echocardiogr 2017;30:303–71.

3. le Polain de Waroux JB, Pouleur AC, et al. Functional anatomy of aortic regurgitation: accuracy, prediction of surgical repairability, and outcome implications of transesophageal echocardiography. Circulation 2007;116 Suppl: I264–9.

KEY WORDS aortic regurgitation, Carpentier classification, echocardiography, mechanisms of aortic regurgitation

APPENDIX For supplemental videos, please see the online version of this paper.